Publication II

Reprinted from Polymer Testing, manuscript accepted for publication 20.4.2006, with permission from Elsevier

Absorption and desorption of water in glass/ethylene-vinyl-acetate/glass laminates

Thomas Carlsson, Petri Konttinen, Ulf Malm, Peter Lund

Abstract:

Ethylene-vinyl-acetate (EVA) is used as the encapsulation polymer in photovoltaic (PV) modules to protect the sensitive parts of the module from the exterior environment. For many module types, exposure to water is an important lifetime-limiting factor. An important question is how quickly the EVA absorbs water in wet conditions and how fast water is desorbed when the module is at operational temperature in sunny conditions. In this work, the water penetration and escape rates in glass/EVA/glass laminates were compared. A question of particular interest was how sample temperature affects the escape rate. It was found that water desorption at 50°C sample temperature is 16 times faster than absorption at room temperature, which implies that unsealed modules will dry out rapidly on sunny days. The implications of water absorption/desorption experiments for module design were also discussed.

Keywords: Ethylene-Vinyl-Acetate, Encapsulation, Absorption, Desorption, Water

1. Introduction

Ethylene-vinyl acetate (EVA) is commonly used as the encapsulation polymer in photovoltaic (PV) modules [1]. A good encapsulation polymer should provide protection from water and impurities, good adhesion to the other components of the module and high transparency. These qualities should remain stable for an expected lifetime of at least 20 years in outdoor use. Additionally, cost and processing considerations are very important. Since it is difficult to find a solution which meets all of these requirements perfectly, it is necessary to know how different encapsulation polymer alternatives meet each criterion so that the necessary compromises can be made. This paper focuses on the behaviour of water in EVA, in particular on how absorption and desorption of water in a PV module can be expected to alternate with the weather conditions.

A standard PV module has an area of 0.5 – 1 m^2 and a thickness of 0.5–2 cm. A common module structure is glass/EVA/photovoltaic cells/EVA/back sheet. The back sheet is sometimes made of glass, but other materials can also be used since transparency is required only on one side of the module. In general, the front and back sheets which give the module rigidity are by far the thickest components of the module, the cells and the encapsulation polymer are both usually less than a millimeter thick.

The front and back sheets of moisture-sensitive PV modules are normally impermeable to water, which makes water penetration through the polymer from the edges of the module the primary water management concern. The edges are often sealed, which reduces water penetration. However, efficient sealing may not always be beneficial. Typical operating temperatures for PV modules in full sunlight are between 50–70°C, so the water which a module has absorbed earlier (in rainy conditions, for example) can desorb from the module to some degree during operation. Even efficient sealing methods allow some absorption of water into the module. If the sealant also

significantly hinders water desorption, the total water exposure of a sealed module may in some situations be higher than that of an unsealed module.

In spite of the importance of water management for PV modules, a number of questions remain unaddressed to date, especially with regard to kinetics of moisture transfer in the encapsulation polymer [2]. This is partly because measurements need to be conducted on laminates with a structure resembling that of PV modules in order to achieve results which are relevant for module design. Commercially available humidity sensors are in general too large to be used inside a laminated structure, and measurement wires may introduce unwanted penetration paths for the water. Through the recent development of a thin moisture sensing element integrated to a glass surface with a TiO_2 film as the moisture-sensitive component [3], non-invasive measurements are now possible for this application.

This study takes advantage of the new moisture sensor and presents a quantitative comparison between the water absorption and desorption rates of laminated EVA at different temperatures. The studied encapsulation scheme is an unsealed glass/ethylene-vinyl-acetate/glass laminate. The diffusion coefficient of water at 25°C in PV-grade EVA (with a vinyl acetate content close to 33%) is in the range 10^{-7}–10^{-6} cm^2/s [4,5] which is a fairly high value compared to other potential PV encapsulant polymers [5]. Water movement in EVA is therefore fairly rapid both in the absorption and desorption phase. The results presented in this paper represent the first absorption/desorption rate comparison for laminated EVA samples.

The temperatures at which absorption and desorption experiments were conducted in this paper correspond to those at which absorption/desorption can be expected to occur in PV modules during real operation. The results indicate that water desorption at module temperatures of 35°C and 50°C is 4 and 16 times quicker than absorption at room temperature, respectively. Since PV modules in most locations spend at least 8-10 hours at temperatures above 50°C on sunny days, significant drying can be expected to occur at the edge of unsealed EVA-encapsulated modules. Moisture-induced damage is therefore expected to occur primarily during extended periods of wet exposure without sunshine.

2. Experimental methods

2.1 Sensor preparation, measurement and lamination

Thin moisture sensors were prepared on indium tin oxide (ITO)-coated glass patterned with photolithographic methods. The ITO pattern for each sensor included an electrode area with two interdigitated fork patterns and conductor lines from the electrodes to the edge of the glass where external conductors could be connected to measure the sensor. Each fork pattern included 14 fingers and each finger was 150 μm wide. Adjacent fingers from opposite sides were spaced 150 μm apart from each other. The sensor was prepared by covering the 3.45mm x 8mm electrode area with Solaronix HT-L TiO_2 paste. After sintering the thickness of the TiO_2 layer was in the range 5±3 μm. The TiO_2 film is porous and it can contain a lot of water relative to its volume. The AC-resistance of the sensor depends exponentially on the water content inside the TiO_2

film. Sensor response is independent of temperature in the range 25°C–85°C and it withstands the standard EVA lamination process [3].

Since manual sensor preparation causes some resistance variation between sensors, a scaled resistance parameter r was defined as

$$r = \frac{\lg(R)}{\lg(R_0)} \quad (1)$$

R is the measured AC-resistance value and R_0 is an AC-resistance value obtained in a weather chamber calibration measurement with the same sensor before lamination. In the calibration measurement, the R of the open sensor was measured at several relative humidity (RH) values, and R_0 was defined as the intersection the linear R vs. RH curve with the RH = 0 axis [3]. In this study lg R_0 was in the range 5.4–5.7 for all sensors, with R_0 expressed in Ω. Sensor impedance was measured with a Zahner IM6 Electrochemical Workstation at frequencies between 1 Hz and 1MHz. All measurements were conducted at zero DC polarization with an AC voltage amplitude of either 200mV or 500mV. The AC-resistance was calculated from the measured spectrum by fitting an equivalent circuit consisting of R in parallel with a constant phase element (CPE) to the measured data. All laminations were carried out in a Panamac L A3-A Automatic PV Module Laminator with 0.5 mm thick EVA (VistaSolar 485.00). The vinyl-acetate content of the EVA was measured to be 33%. Sensor preparation, measurement and calibration have been presented and discussed in detail elsewhere [3]. Since the sensor is prepared on the glass surface, the structure of the finished samples was glass/sensor/EVA/glass.

2.2 Absorption and desorption experiments

In order to use the moisture sensor in desorption experiments, a verification of its behaviour during desorption was needed to confirm that the water does not remain locked inside the TiO_2 film when the EVA on top of it dries out. For this purpose, absorption and desorption experiments were first performed without a top glass in a glass/sensor/EVA configuration in Arctest ARC-150 and ARC-400 weather chambers. Two samples were tested, one at 25°C and the other one at 50°C. The water concentration in the EVA was first allowed to saturate at an initial RH level. Saturation was judged by the moisture sensor response, a nearly constant r indicating that the sensor, the EVA and the surrounding environment were near equilibrium. From a given state of sufficiently stable equilibrium, the RH was changed rapidly to a new value and sensor response was measured during the transition. As the external RH changed, the water concentration in the EVA also changed through inward or outward water diffusion depending on whether RH was increased or decreased. This changed the water concentration in the sensor as a new equilibrium was approached. The purpose of the experiment was to determine whether the sensor exhibits any time lag in responding to changes in water concentration in the EVA. If the sensor reacts equally quickly to a step from high to low RH as it does to an RH change in the opposite direction at the same temperature, then water moves freely out of the sensor when the EVA dries out and

sensor response gives information on the desorption rate. The RH cycle was 70%–90%–70% at 25°C and 60%–70%–80%–90%–60% at 50°C.

In the main part of this work, glass/sensor/EVA/glass samples were studied. The top glass had to be smaller than the bottom glass to accommodate electrical contacting to the edge of the ITO-patterned bottom glass. Figure 1 illustrates the positioning of the sensors and the contacts to which external leads were connected. The bottom glass was 100mm x 100mm in size with the etched ITO pattern shown in grey colour. TiO_2 was applied to the sensor areas numbered I-VI. The distance between the sides of adjacent sensors was 5mm or 6mm depending on location. The top glass and the EVA layer laminated beneath it were 90mm x 90mm in size. Both the top and bottom glass sheets were approximately 1 mm thick. During lamination the top glass was kept in place above the bottom glass with a copper frame. The EVA which had been squeezed out beneath the edges of the top glass was removed with a scalpel after lamination. The edges marked with B in Fig. 1 were sealed to allow water penetration only through edge A. The distances from the sensor edges to the top glass edge A, which equalled the required water penetration depth to reach the sensors, were approximately 2 mm for sensors III and IV, 4 mm for II and V, and 6 mm for sensors I and VI, respectively. The positioning of the top glass and the distance from the sensors to the glass edge varied approximately ±0.5mm between the samples.

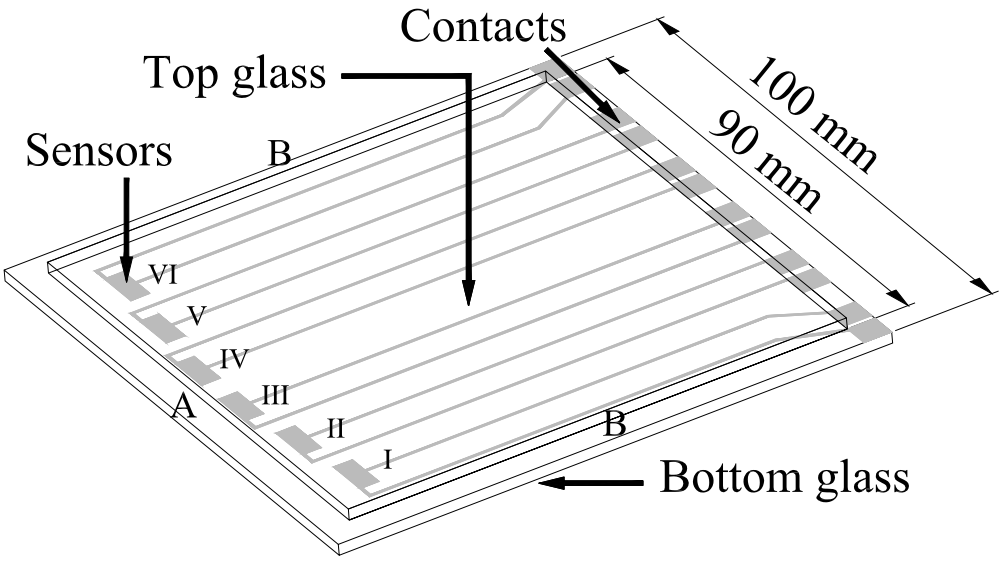

Figure 1. *Laminated glass/EVA/glass sample for absorption/desorption experiments. Sensors are numbered from I to VI and ITO contact squares for measurement leads are indicated.*

When water penetrates the encapsulation from the sample edge A and reaches the TiO_2 film, it probably fills out the TiO_2 film approximately uniformly because water moves easily in the porous TiO_2 material. Water movement in the EVA is expected to be significantly slower. The detailed mechanisms of sensor filling are not of critical importance for the results in this paper, but some remarks on expected sensor behaviour are in order. The porosity of the TiO_2 was about 50%, which means that the 5

μm thick TiO_2 layer can hold on the order of 2.5 μg/mm^2 of water when all pores are filled. The water saturation concentration of EVA with 33% vinyl acetate content is 5 μg/mm^3 [4], which means that in a state of complete saturation the amount of water in the TiO_2 is comparable to the amount of water in the 0.5 mm thick EVA layer. It is therefore likely that the TiO_2 film acts as an effective sink for the water which penetrates the EVA. The points made above indicate that water enters the sensor mainly at the outer edge of the TiO_2 film. During the experiments described below, sensors I, II, V and VI did not give measurable signals. Since the width of all sensors (3.45 mm) was larger than the difference in distance to edge between sensor pairs II/V and III/IV (2 mm), it can be concluded that the water front in the EVA probably did not penetrate past the surface area of sensors III and IV. This being the case, the response from sensors III and IV followed directly from the inward and outward movement of water at the edge, and gave a valid comparison between the water absorption and desorption rates.

During water absorption half of the sample was immersed in a bath of distilled water at room temperature (22–25°C) and sensor response was logged as water absorption proceeded at edge A. The experimental setup corresponds roughly to the situation in field conditions when water penetration is likely, i.e. on cloudy and rainy days when module temperature is equal to ambient temperature. Absorption experiments were followed by desorption measurements on a hot plate at both 35°C and 50°C and on the table at room temperature. The surroundings in the desorption experiments were normal room conditions (22–25°C, RH 20–50%). On sunny days PV modules in the field regularly reach temperatures clearly above 50°C for extended periods of time, so the experimental setup approximates the real desorption conditions outdoors.

3. Results

3.1 Verification of sensor behaviour

Figure 2 shows the measured sensor response at 25°C in a glass/sensor/EVA structure exposed to the relative humidity changes indicated by the solid line. The RH in the weather chamber oscillated around the set values within the limits 90 ± 2% and 70 ± 1.5% during the experiment. The data on the weather chamber curve during and immediately after each abrupt change in RH is shown as measured, but the remaining part of the curve at constant RH has been straightened manually to maintain clarity in the figure. The RH oscillation did not have any effect on sensor response, because short-term variations (with a period of approximately 2 minutes) were averaged out as the water diffused through the EVA to the sensor.

Sensor absorption response in Figure 2 shows that it takes 15-20 hours before the sensor is close to a new equilibrium after the RH step. It can be seen that the desorption process occurred at approximately the same rate as absorption after a small initial delay. In the upward step from 70% to 90% RH, the first signs of change in sensor response were detected about 20 minutes after the step. In the downward step from 90% to 70% RH, changes were observed after 50 minutes. Figure 3 shows the same measurement for a different sensor at 50°C with several upward RH steps. In this

case, the diffusion process is quicker and the first changes in sensor response are observed after 1-2 minutes in each absorption phase and within 7 minutes in desorption. The sensor response curve has a slightly longer time constant in the drop from RH 90% to 60% than in the upward RH steps. This is explained by the slowness of the weather chamber in the downward step (17 minutes was needed to complete this step, compared to 2-3 minutes in the upward steps).

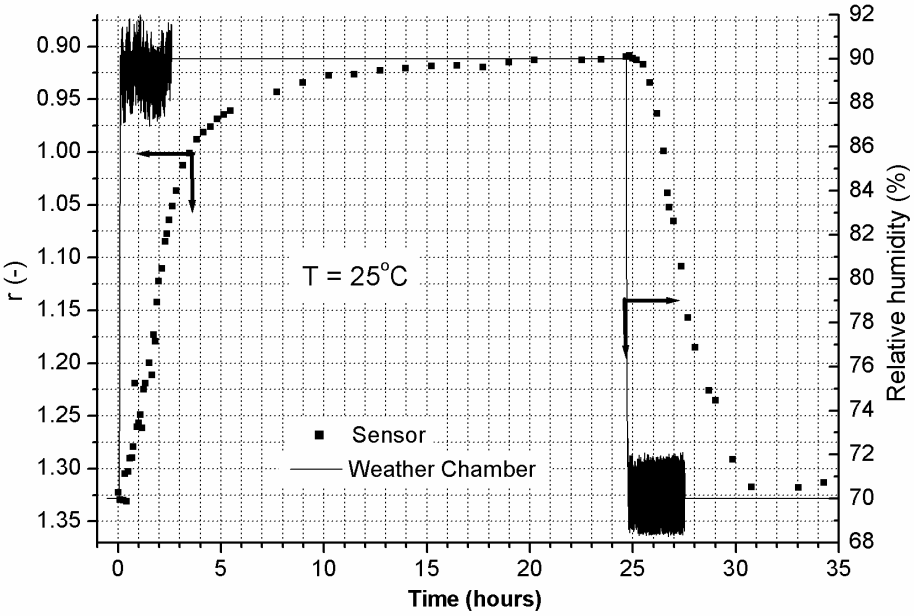

Figure 2. *Weather chamber measurement to verify sensor response to water absorption and desorption at 25°C. The delay is slightly longer in desorption than in absorption, but the difference is insignificant for the purposes of this study. RH curves have been partially modified to maintain clarity.*

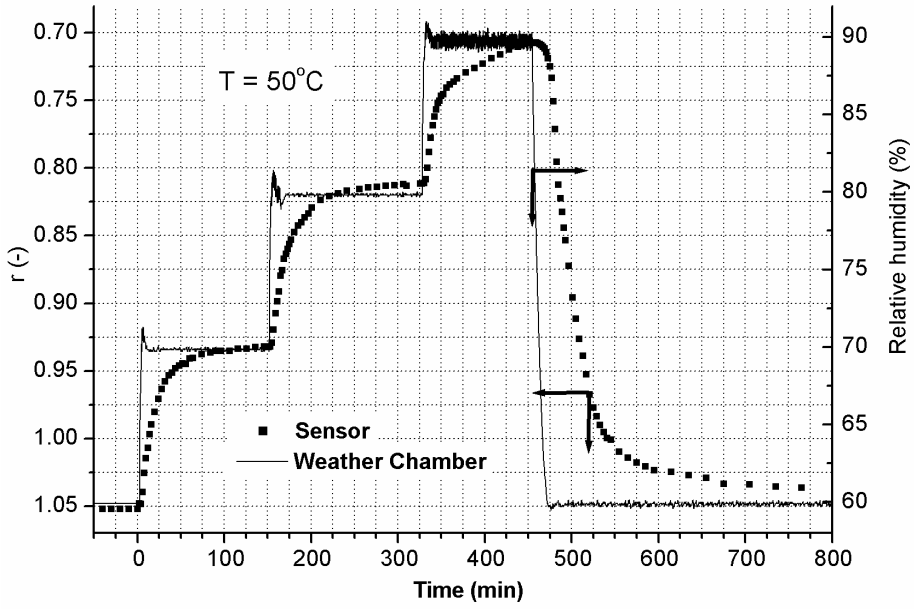

Figure 3. *Weather chamber measurement to verify sensor response to water absorption and desorption at 50°C. Desorption is delayed slightly more than absorption, but the difference is insignificant for the purposes of this study.*

As seen in Figure 3, the step from 80% to 90% at 50°C resulted in a differently shaped curve in the r(t) data compared to the other steps at this temperature. A possible explanation for this is that the accuracy of the fit calculated to the measured AC-spectrum was reduced by the large amount of water present in the TiO_2 at RH values above 80. While this brings some uncertainty to this experiment, the onset of desorption is still clearly visible in Figure 3. Additionally, it will be observed that sensors did not approach equally low values for r in the actual absorption/desorption experiments described below, so a similar loss of accuracy was not expected there. The time scales of interest in the absorption/desorption tests for glass/EVA/glass samples were over 1 hour at 50°C and over 10 hours at room temperature. The small delays in response evidenced by the data in Figures 2 and 3 have insignificant effects on the results of the experiments performed in this work. It can therefore be concluded that the sensor works as required at both temperatures.

3.2 Absorption and desorption from glass/EVA/glass laminates

The results presented here are all from sensors closest to edge A, labelled with III and IV in Figure 1. Sensors further away from the edge did not register measurable signals during the experiments. Figure 4 shows the time series of sensor response r in consecutive absorption and desorption measurements for two laminated glass samples, S1 and S2. In both samples, the measured sensors were accompanied by a second sensor at the same distance from the edge. These reference sensors mirrored the behaviour of the primary sensors closely. The precise distance of the TiO_2 film edge from the glass edge was 1.6 mm in S1 and 2.4 mm in S2. The logarithm of R for the sensor in S1 is shown on the right axis to indicate the magnitude of the measured resistance values. The time scale shows the number of elapsed hours since the beginning of the experiment when the samples were put in the water bath for the first time.

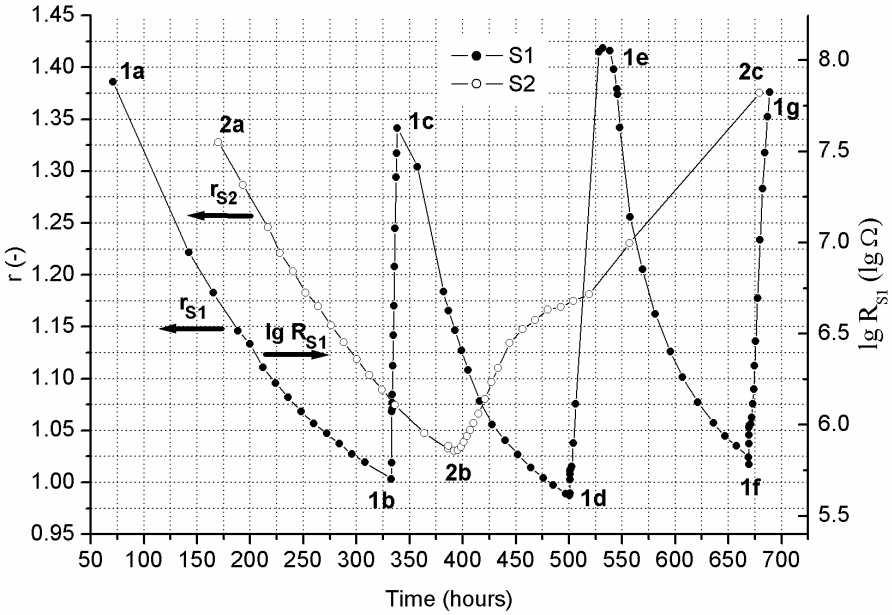

Figure 4. *Complete series of measurement data from consecutive absorption and desorption experiments with samples S1 and S2. To exemplify the measured resistance values, the lgR axis for the sensor in sample S1 is shown on the right.*

Sample S1 went through the following sequence: 1a) absorption of water at room temperature, first sensor response obtained after ~75h, 1b) start of first desorption at 50°C sample temperature, 1c) start of second absorption at room temperature, 1d) start of second desorption at 35°C sample temperature, 1e) start of third absorption at room temperature, 1f) start of third desorption at 35°C sample temperature, and 1g) end of experiment. The second desorption lacks data points due to a measurement error. The third desorption was therefore also conducted at 35°C to gather sufficient data. Each desorption was continued until the sensor reached resistances corresponding to approximately r = 1.3 – 1.4, which is close to the maximum measurable resistance. The samples were not dried out completely in the desorption phase because it would not have been possible to determine when drying is complete. Stopping the desorption at a specific r value enabled controlled repetition of the absorption experiment with a well-defined starting point. Sample S2 underwent 2a) absorption of water at room temperature, with the first signals measured from the sensor after 175h, 2b) desorption of water at room temperature, and 2c) end of experiment. The time difference between the first absorption curves of S1 and S2, with S2 reaching a given r value about 75h after S1, is due to the difference in the distance from the sensor to the edge of the glass.

To gain insight into changes in the absorption rates during multiple cycles, the different absorption phases of sample S1 in Figure 4 have been plotted together in Figure 5. The time axis of the second and third phase absorption data was chosen so that the curves passed through the same point, denoted by a in Figure 5. This enables a direct comparison of the absorption rate from that point onward. It is observed that the second absorption is significantly faster than the first one, reaching r = 1.00 in approximately half the time. The third absorption occurs very nearly at the same rate as the second one. The 2nd and 3rd curves can thus be taken as an initial approximation of the absorption rate after a few absorption/desorption cycles.

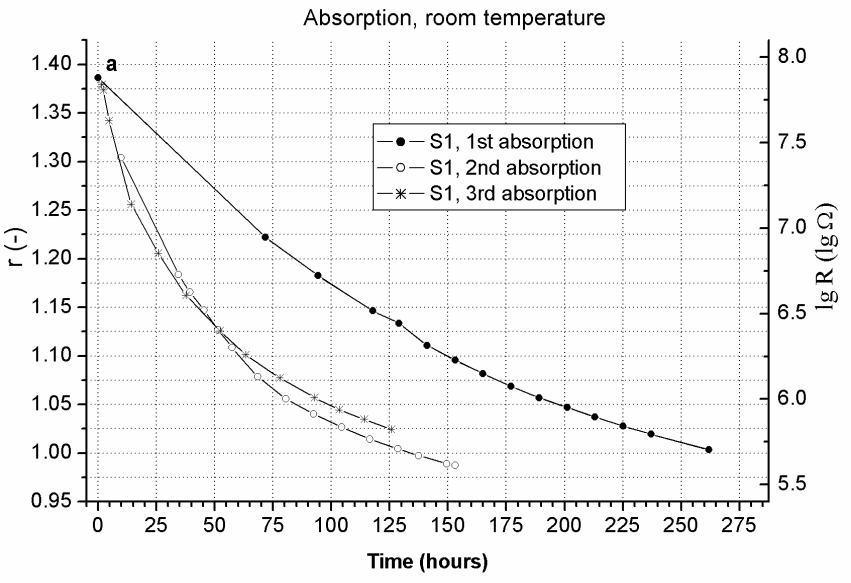

Figure 5. *Comparison of absorption rates in the first, second and third absorptions into sample S1 in Figure 4. The first absorption proceeds slower than the following ones.*

Two of the desorption phases of S1 and the desorption phase of S2, in Figure 4, are shown together in Figure 6, where the zero-point time corresponds to the time of removal from the water bath (and, in the case of high temperature tests, placement of the sample on the hot plate). It is observed that the desorption rate is a very sensitive function of sample temperature. At 50°C the sample returns from r = 1.05 to r = 1.35 in 5 hours, at 35°C the same process takes about 20 hours. The desorption curve of S2 is not shown in its entirety in Figure 6, but is visible in Figure 4. A precise comparison between S1 and S2 should take into account that the S2 sensor was further from the edge, but it can be remarked that desorption in S2 occurs approximately at the same rate as absorption, taking about 260 hours to return from r = 1.05 to r = 1.35. A clear desorption plateau is seen in S2 and also in both desorption curves from S1. This behaviour may be either due to the desorption characteristics of water from EVA or to sensor behaviour. Absorption and desorption processes are compared in Table 1, where the times needed for the transition between r = 1.05 and r = 1.35 are presented for each absorption/desorption phase. At a 50°C module temperature, desorption from S1 occurs 16 times faster than absorption at ambient temperature and desorption at 35°C is at least four times as quick as ambient absorption. The question of how repeated cycling affects the desorption rate was not studied in this work.

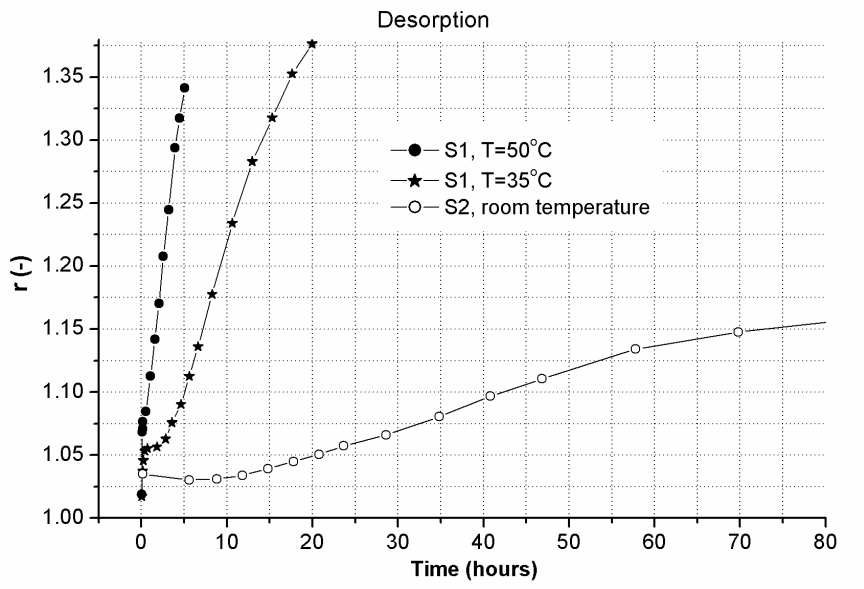

Figure 6. *Comparison of desorption curves at different sample temperatures for S1 and S2. Surroundings were at room temperature in all experiments.*

***Table 1**: Comparison of absorption and desorption times for 1st, 2nd and 3rd absorption cycles in sample S1 and desorption times at different sample temperatures in samples S1 and S2. The table presents the time needed for the transition between r = 1.05 to 1.35.*

#	Absorption	T_{sample}	Desorption
1st	182 h (S1)	room	260 h (S2)
2nd	81 h (S1)	35°C	20 h (S1)
3rd	95 h (S1)	50°C	5 h (S1)

4. Summary and discussion

The purpose of this paper was to quantify the difference in water absorption and desorption rates at the edge of photovoltaic modules encapsulated with ethylene-vinyl-acetate without edge sealing. Absorption occurs in conditions where the module is at ambient temperature, desorption when module temperature is above ambient temperature. In a basic glass/EVA/glass encapsulation without framing, even a 10–13°C difference between the module and ambient temperatures is enough to drive out water 4 times faster than the rate of penetration. When the module temperature is 25–28°C higher than the surroundings, the desorption rate is 16 times higher than the earlier rate of absorption. For this reason it is plausible to assume that unsealed, EVA-encapsulated modules should frequently dry out in the summer when high module temperatures are reached repeatedly for long time periods. The water exposure of a module will depend strongly on how often wet and sunny conditions alternate in the climate where it is used.

The method used in this paper can be directly applied to the study of water absorption/desorption in laminates with alternative encapsulation polymers and/or different edge sealing alternatives. Most encapsulation polymers can be expected to behave similarly to EVA, except that the area of the module which is exposed to repeated moisture penetration and escape will depend on the water diffusion coefficient. The design of the PV module edge, especially with regard to the distance of the nearest photovoltaic cells from the module edge and to the sensitivity of the entire module to edge-cell damage, is an important determinant of its moisture stability. Edge sealing further extends the possibilities of encapsulation design. Measurement of water absorption and desorption in field conditions should provide interesting comparisons. It is possible that the optimal encapsulation solution for PV modules which are used in locations with long and wet winters is significantly different from the optimum for sunnier climates. Finally, it should be remarked that the results obtained in this paper were from unaged samples. In long-term outdoor usage aging mechanisms [1,6] may change the absorption/desorption characteristics of EVA and other encapsulants. This is an important question to address in future studies on this topic.

References

1. A.W. Czanderna and F.J. Pern. Sol.En.Mater.Sol.Cells 1996; 43(2): 101-181.

2. T.McMahon. Prog.Photovolt. 2004; 12(2-3) 235-248.

3. T.Carlsson, J.Halme, P.Lund, P.Konttinen. Sens. Actuators A 2006; 125 (2): 281-287.

4. S. Marais, Y. Hirata, D. Langevin, C. Chappey, T. Nguyen, M. Metayer. Mat.Res.Innovat. 2002; 6(2): 79-88.

5. M.Kempe In: Conference Record of the 31st IEEE Photovoltaic Specialist Conference, Orlando, 2005. p. 503-506.

6. P.Klemchuk, M.Ezrin, G.Lavigne, W.Holley, J.Galica, S.Agro. Polym.Degr.Stab. 1997; 55(3): 347-365.